JACS
JOURNAL OF THE AMERICAN CHEMICAL SOCIETY
Communication
pubs.acs.org/JACS

Unique Lead Adsorption Behavior of Activated Hydroxyl Group in Two-Dimensional Titanium Carbide

Qiuming Peng,*[,†,#] Jianxin Guo,[†,#] Qingrui Zhang,*[,‡] Jianyong Xiang,[†] Baozhong Liu,[§] Aiguo Zhou,[§] Riping Liu,[†] and Yongjun Tian[†]

[†]State Key Laboratory of Metastable Materials Science and Technology, [‡]Hebei Key Laboratory of Applied Chemistry, School of Environmental and Chemical Engineering, Yanshan University, Qinhuangdao 066004, PR China

[§]School of Materials Science and Engineering, Henan Polytechnic University, Jiaozuo 454000, PR China

Supporting Information

ABSTRACT: The functional groups and site interactions on the surfaces of two-dimensional (2D) layered titanium carbide can be tailored to attain some extraordinary physical properties. Herein a 2D alk-MXene ($Ti_3C_2(OH/ONa)_xF_{2-x}$) material, prepared by chemical exfoliation followed by alkalization intercalation, exhibits preferential Pb(II) sorption behavior when competing cations (Ca(II)/Mg(II)) coexisted at high levels. Kinetic tests show that the sorption equilibrium is achieved in as short a time as 120 s. Attractively, the alk-MXene presents efficient Pb(II) uptake performance with the applied sorption capacities of 4500 kg water per alk-MXene, and the effluent Pb(II) contents are below the drinking water standard recommended by the World Health Organization (10 μg/L). Experimental and computational studies suggest that the sorption behavior is related to the hydroxyl groups in activated Ti sites, where Pb(II) ion exchange is facilitated by the formation of a hexagonal potential trap.

Heavy metal pollution in waters is a worldwide and serious environmental issue due to their toxicity and carcinogenicity. Some toxic metals are dangerous even at trace amounts. Various technologies including chemical precipitation,[1] membrane,[2] adsorption,[3] and electrodialysis[4] are well developed for trapping toxic metals from water. Among the available methods, adsorption is one of the most attractive options.[5] Two-dimensional (2D) materials with large surface areas and abundant active sites have been exploited as ideal adsorbents for environmental remediation. Significantly, graphene oxide (GO) and its derivatives, prepared from chemical oxidation of natural graphite,[6] have garnered its fair share of interest for its potential for the extraction of heavy metal,[7] arsenate,[8] organic dyes,[9−11] and bisphenol from water.[12] However, its simple chemistry with only carbon networks, the weak van der Waals bonding between adjacent layers in multilayer structures, especially the large strong acid/oxidant consumption, as well as low production efficiencies have slowed down their use in such applications.

Recently, a large family of 2D materials, labeled MXene, has stimulated research enthusiasm, because they combine hydrophilic surfaces, good structural and chemical stabilities, excellent electrical conductivities, and environment-friendly characteristics. MXenes are a group of layered 2D materials,[13−16] produced by immersing Al-containing, $M_{n+1}AX_n$ (n = 1, 2, 3), or MAX phase (where M represents an early transition metal, A corresponds to III A or IV A group elements, and X is C or N) powders in HF solutions at ambient temperatures. This facile one-step synthesis is eminently scalable and could be produced at large enough scales for engineering applications.

To date the most studied MXene is Ti_3C_2, prepared by immersing Ti_3AlC_2 in HF at room temperature. It was shown that a host of cations, such as Li^+, Na^+, Mg^{2+}, K^+, and NH_4^+ are readily and spontaneously intercalated between the Ti_3C_2 layer in aqueous solutions.[6] This discovery paves the way for the use of these materials in energy devices such as supercapacitors,[13] Li-batteries,[17,18] and hydrogen storage.[19] Little is known, however, about possible applications for environmental pollutant decontamination. In general, titanium (Ti) has high sorption affinity toward metallic ions, especially heavy metals.[20−24] In the MXene the exposed titanium surfaces are initially terminated by OH or F group after exfoliation, resulting in the formation of Ti−OH and Ti−F bonds. And then cation substitution on hydroxyl group can obtain some ion-change sites, which might provide preferential sorption of toxic metals, in which the layered structure of the MXene with large surface areas enhances sequestration of target metal-pollutants.

Herein, we found that the hydroxyl terminated Ti-surfaces treated with alkalization intercalation exhibit unique adsorption behavior. The sorption performance and mechanism of heavy metals onto alk-MXene ($Ti_3C_2(OH/ONa)_xF_{2-x}$) phase are revealed by a series of structural characterization and batch sorption runs. Lead (Pb) was selected as a model toxic metal because of its high toxicity and carcinogenicity and because it is listed as a priority heavy-metal pollutant by most national environmental protection agencies.

A typical exfoliation and alkalization process of layer-shaped Ti_3AlC_2 powders was observed by SEM (Figure S1, Supporting Information (SI)). The average dimension of the starting Ti_3AlC_2 particles is ~3 μm. The gaps are first produced at the edges of powders, and then spread along the surface with prolonging immersion. After immersion for 10 h, open arch-shaped edges at the ends of MXene layers resembled to graphene were observed (Figure 1A). The wide gaps are 50−100 nm in

Received: January 16, 2014
Published: March 3, 2014

dx.doi.org/10.1021/ja500506k | J. Am. Chem. Soc. 2014, 136, 4113−4116

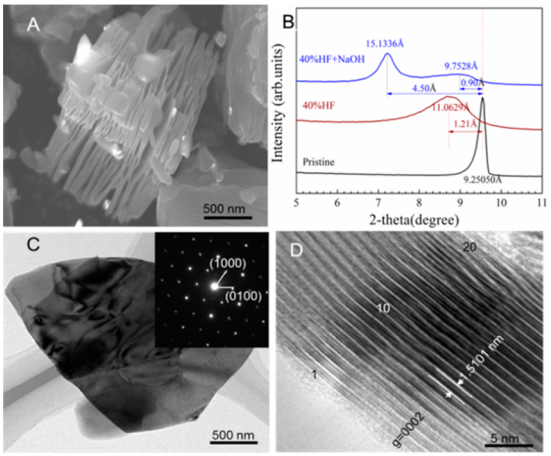

Figure 1. (A) SEM graph of alk-MXene material after exfoliating for 10 h in HF solution. (B) The XRD patterns of different state samples. (C) The TEM micrograph of alk-MXene sample. The inset is the selected area electron diffraction along [0001] direction. (D) HTEM micrograph of alk-MXene.

size, and the sheets consist of MXene layers containing OH and F groups. After alkalization treatment, the sample shows the similar morphology with wider gaps (Figure S1D).

This process is confirmed by XRD observation (Figure S2A and Figure 1B) and EDX elemental compositions (Figure S1 and Table S1). Both the elimination of the (104) peak of containing Al (~39°) reveals the loss of Al after immersion in HF solution.[25] Additionally, the (002) peak shifts toward low angle direction after NaOH treatment, suggesting the occurrence of intercalation of Na ions. In the case of EDX results, the peak of Al disappears after immersion for 4 h. The reduction of F peak together with the presence of Na peak demonstrates that the alkalization process is of benefit to the transformation of F group to OH group and the intercalation of Na ions. TEM micrograph (Figure 1C) shows that the alk-MXene sample, henceforth referred to as ($Ti_3C_2(OH/ONa)_xF_{2-x}$), maintains the hexagonal structure of the parent MAX phase. The multilayer stacks are not homogeneous, but are comprised of ~20 layers each (Figure 1D). The layer spacing along the *c*-axis is about 1.5101 nm (Figure 1C).

Series batch tests for adsorption performances toward toxic Pb(II) ions onto alk-MXene were performed using the bottle-points methods.[26] The Pb(II) uptake is a pH-dependent process (Figure S3). The increase in pH value exhibits preferential sorption performances with the optimum pH ranging from 5 to 7. After the Pb adsorption treatment (pH = 6.5), some fine particles were found on the surface of alk-MXene (Figure S4). Finally, a flocculence layer composed of Pb, Ti, O, F, and Na elements is detected. Such pH-dependent adsorption indicates the Pb(II) uptake behaviors onto alk-MXene might be the ion-exchange behaviors in nature because of the presence of [Ti−O]$^-$H$^+$ and [Ti−O]$^-$Na$^+$ groups.[27] The negligible Pb(II) sequestration in low pH (pH < 1) suggests the alk-MXene material could be regenerated by acidic solutions.[3]

In addition, the common cations, particularly for Ca(II) and Mg(II) are always ubiquitous in natural water and wastewater effluents. The same positive-charge and high level contents might lead to serious sorption competition toward Pb(II) or other heavy metals removal. Thus, it is of particular significance to elucidate the sorption selectivity of alk-MXene toward Pb(II) retention with the coexistence of common cations. The commercial polystyrene ion-exchange resin 001x7 with sulfonic acid groups was used for a reference. Figure 2A,B reveals that the

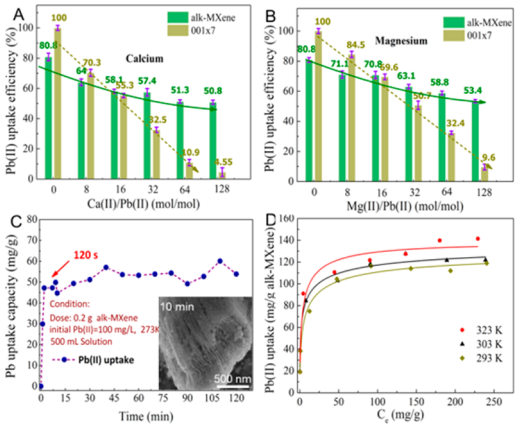

Figure 2. (A,B) Effect of competitive ions on uptake of lead ions onto alk-MXene and 001x7 (A) calcium ions, (B) magnesium ions (0.5 g/L adsorbent initial Pb(II) = 0.25 mM, pH = 5.8−6.2). (C) Lead sorption kinetics tests and SEM morphology. (D) Temperature-dependent lead sorption isotherms onto alk-MXene.

Ca(II)/Mg(II) addition resulted in a decreased adsorption trend for both alk-MXene and 001x7. Comparatively, the alk-MXene still exhibit outstanding Pb(II) uptake behaviors. The removal of Pb(II) from a solution containing above 16 times Ca(II) and Mg(II) cations was slightly influenced by the presence of the competing cations. The same solution, on the other hand, severely reduced, to near zero, the sorption of Pb(II) by 001x7. It is noteworthy that the sulfonate groups within 001x7 sequester the Pb(II) ions mainly through nonspecific electrostatic interactions. The latter are clearly not selective to Pb(II) but also clearly adsorb the Ca(II)/Mg(II) ions as well.

It follows that the selectivity of the MXene material to Pb(II) is significantly higher than that of the 001x7. We ascribe this selectivity to three reasons: (i) The surface [Ti−O]$^-$H$^+$ groups exhibit strong metal−ligand interaction with Pb(II) ion in aqueous solutions and increase the sorption selectivity. Such remarkable affinities are the so-called "inner-sphere complexation", which has been demonstrated by Brown and Giammar's research.[28,29] (ii) The laminate nanostructure produced by HF exfoliation possesses large surface areas (maximum ~484 m^2/g[14]). Both [Ti−O]$^-$H$^+$ and [Ti−O]$^-$Na$^+$ sites are believed to be favorable for the enhancement of Pb(II) uptake to form Ti-OPb. In addition, with the decrease of F group and the increase of OH group, this adsorption role is further strengthening. (iii) In general divalent cations are always sorbed preferably with low hydration energies.[30] The Gibbs free energies of hydration are −1425 kJ/mol for Pb(II), −1505 kJ/mol for Ca(II), and −1830 kJ/mol for Mg(II).[31] The low hydration energy of Pb(II) suggests the preferential adsorption and the selective sequence as Pb(II) > Ca(II) > Mg(II), which agrees with the experimental results.

To gain further insight into sorption mechanism, FT-IR spectrum and XPS analysis of alk-MXene before and after Pb(II) ion loading were performed. The FT-IR spectra (Figure S5) confirm the presence of external water in addition to the strongly hydrogen-bonded OH or extremely strongly coordinated H_2O by the sharp peaks at ~3431 and ~1628 cm^{-1}; the peaks at 598 cm^{-1} might be assigned to the deformation vibration for the Ti−O bond.[32] After the adsorption of Pb(II) ions, the Ti−O peak

dx.doi.org/10.1021/ja500506k | J. Am. Chem. Soc. 2014, 136, 4113−4116

splits into two sharp absorption peaks at ~653 and ~618 cm^{-1}, indicating the formation of Pb−O and Ti−O interaction.[32] The large shifts of Ti−O band after Pb(II) loading demonstrates the presence of strong affinities between Ti−O and Pb(II) ions, which might result from inner-sphere complex formation onto the surface of alk-MXene.

The presence of distinct Na 1s sharp peak centered at 1072.1 eV on alk-MXene in the XPS spectra (Figure S6) suggests the success intercalation of Na(I). Comparatively, the distinguished Pb 4f binding energy peaks, and negligible Na 1s peaks further demonstrate the sorption of Pb(II) and Na(I) replacement corresponding to the same sorption sites. Note that the Pb(II) binding energies for purified $Pb(NO_3)_2$ are centered at 144.5 eV for Pb $4f_{5/2}$ and 139.6 eV for Pb $4f_{7/2}$, respectively. For Pb(II) loaded alk-MXene samples, a remarkable shift of 0.8 eV to lower binding energy of Pb 4f was observed. This shift indicates the formation of strong affinities between the Pb(II) ions and alk-MXene. Similar shifts, of 0.4 eV, were concomitantly observed for the Ti 2p (Figure S6C) and O 1s (Figure S6D), confirming the possible strong interaction between Ti−O and Pb(II) ions.

Kinetic experiments were carried out by determining the solution Pb(II) contents at various time intervals. Surprisingly, the sorption equilibrium was achieved within 120 s (Figure 2C). These rapid kinetics are mainly attributed to the unique layered nanostructure of alk-MXene, which could favor for the accessibility of Pb(II) intercalation and diffusion. In addition, sorption isotherms (Figure 2D) reveal that the alk-MXenes show larger sorption capacities (~140 mg/g) as compared to other Pb(II) adsorbents roughly (Table S2). Considering 20 layers (Figure 1D), the maximum theoretical adsorption capacity is ~2800 mg/g. Such temperature dependence of favorable adsorption equilibrium illustrates that the Pb(II) uptake onto alk-MXene is driven by ion-exchange process spontaneously and the adsorption interaction with Pb(II) is an endothermic reaction.[33]

Figure 3 illustrates an effluent history of alk-MXene treatment for drinking water containing the Pb(II) ions. The layered

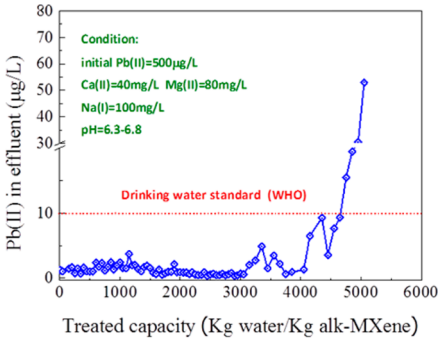

Figure 3. Treatment capacity of layered alk-MXene for simulated lead contaminated drinking water with an initial concentration of 500 μg/L.

material alk-MXene displays excellent sorption performances, and the average water treatment capacities are 4500 kg of water/kg of alk-MXene before significant degradation in sorption capabilities. Such efficient Pb(II) adsorption leads to effluent contents <2 μg/L, which clearly meets the drinking water standard recommended by WHO (10 μg/L). The obtained alk-MXene-Pb presents excellent solid−liquid separation properties for five minutes (Figure S7), which suggests their potential applications. Moreover, the exhausted materials are amenable to efficient regeneration by the binary 0.1% HNO_3 + 5% $Ca(NO_3)_2$ solution with the desorbed Pb(II) efficiency of 95.2%.

The adsorption behavior is elucidated by first principle calculations. The exposed titanium surfaces are terminated by OH or F group after exfoliation, whereafter the partial F groups changes to OH ones and the OH groups transforms to ONa ones after alkalization treatment. The different Pb coverages (Θ) per monolayer (ML) are considered (Figure S8) to confirm the possible Pb replaced occupation. To understand the stability of Pb occupation in alk-MXene ($Ti_3C_2(OH/ONa)_xF_{2-x}$), the model of formation energies, ΔH, is supposed, where the effect of fluorine groups is not considered because of low concentration and negative charge. The possible chemical reactions are shown as follows:

$$Ti_3C_2(OH)_2 + Pb(NO_3)_2 \rightarrow Ti_3C_2(O_2H_{2-2m}Pb_m) + HNO_3 \quad (1)$$

$$Ti_3C_2(ONa)_2 + Pb(NO_3)_2 \rightarrow Ti_3C_2(O_2Na_{2-2m}Pb_m) + NaNO_3 \quad (2)$$

In the case of adsorption process, two reactions occur concurrently (Table S3), and both equations reveal the same ion change mechanism. Considering the high ratio of H:Na (~5.75, Table S1), it is believed that the eq 1 acts as the dominated one during adsorption. Herein, taking eq 1 as a sample, we interpret the adsorption behavior in detail. ΔH is defined as the following:

$$\Delta H_{(Ti_3C_2(O_2H_{2-2m}Pb_m))} = E_{tot(Ti_3C_2(O_2H_{2-2m}Pb_m))} + 2mE_{tot(HNO_3)} - E_{tot(Ti_3C_2(OH)_2)} - mE_{tot(Pb(NO_3)_2)} \quad (3)$$

where E_{tot} are the total energies of corresponding substances, which are calculated in this work. According to this definition, a negative ΔH indicates that it is energetically favorable for given reagents to form more stable products and vice versa. The same method applied to the reaction of $Ti_3C_2(OH)_2$ and $Mg(NO_3)_2$ or $Ca(NO_3)_2$. The Θ (1/9, 1/16) of $Ti_3C_2(O_2H_{2-2m}Pb_m)$ is stable since the formation energy is negative (Table S3), indicating that occupation of Pb in $Ti_3C_2(O_2H_{2-2m}Pb_m)$ occurs by substituting two H atoms of $Ti_3C_2(OH)_2$ when the Pb coverage is less than 1/4. However, in the cases of Ca(II) and Mg(II) ions, the negative value of Θ corresponds to 1/16, revealing that the alk-MXene is more selective to Pb(II).

The valence electron localization function (ELF) provides the bonding information by measuring electron localization in atomic and molecular systems.[34] The hydroxyl groups around Pb atom and oxygen atom under Pb atom together constrain the adsorbed Pb atom to form a hexagon hydroxyl potential trap (Figure 4 and S8). A majority of surface electrons of $Ti_3C_2(O_2H_{2-2m}Pb_m)$ are located in the vicinity of Pb atom (Figure 4A−D) except for a few lone pair electrons. The Pb atom forms stronger bonds with hydroxyl around Pb atom than oxygen atom under Pb atom (hydroxyl of losing H atom) in $Ti_3C_2(O_2H_{2-2m}Pb_m)$. It shows that the adsorption of Pb is more associated with the hydroxyl, which is consistent with the result that the interaction of oxygen atom (hydroxyl of losing H atom) with Ti_3C_2 are stronger than that of oxygen atom of hydroxyl in $Ti_3C_2(O_2H_{2-2m}Pb_m)$.

There is an obvious hybridization between Pb atom and $Ti_3C_2O_2H_{2-2m}$. The Pb 5d-orbitals (Figure 4Ea) form the energy bands hybridized with O 2s-orbitals (Figure 4Eb) (between −17.0 and −20.0 eV), with O 2p- and H 1s-orbitals (Figure 4Ed,Ef) of hydroxyl close to Pb atom (between −8.0 and −10.0 eV). Conversely, there are no change for projected density of states (PDOS) between H/O atom far from Pb atom (Figure

dx.doi.org/10.1021/ja500506k | J. Am. Chem. Soc. 2014, 136, 4113−4116

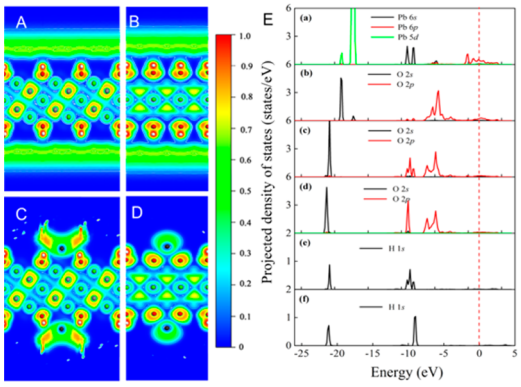

Figure 4. ELF slices (A–D) and PDOS (E) of $Ti_3C_2(O_2H_{2-2m}Pb_m)$ for 1/9 ML. (A) and (B) are (110) plane and (−110) plane ELF slices of pristine $Ti_3C_2(OH)_2$, respectively. (C) and (D) are (110) and (−110) plane ELF slices of $Ti_3C_2(O_2H_{2-2m}Pb_m)$, respectively. (Ea) Pb atom; (Eb) O atom close to Pb atom (hydroxyl losing H atom); (Ec) O atom of hydroxyl close to Pb atom; (Ed) O atom of hydroxyl far form Pb atom; (Ee) H atom of hydroxyl close to Pb atom; (Ef) H atom of hydroxyl far from Pb atom.

4Ed,Ef) and H/O atom of pristine $Ti_3C_2(OH)_2$, suggesting that the hybridization of Pb atom and $Ti_3C_2O_2H_{2-2m}$ originates mostly from Pb atom and its nearer hydroxyl and O atom. The interaction of Pb atom and hydroxyl far from Pb atom is too small to may be ignored. In addition, the insertion of Pb atom renders the electrons (or electron states) of Ti and C atoms of $Ti_3C_2(O_2H_{2-2m}Pb_m)$ to redistribute (Figure S9), which corresponds to the little change of Fermi energy of total density of states (Figure S10).

In conclusion, we have developed an exfoliation and alkalization–intercalation method for the large-scale synthesis of functional 2D-MXene materials. The layered structure and abundance in activated Ti–OH sites offer potential applications toward Pb(II) purification for environmental remediation. The alk-MXene exhibits large sorption capacities, fast kinetic, extremely trace Pb(II) effluent, and reversible adsorption properties. The method is highlighted by its simplicity and high-yield production of a well-defined morphology, which is promising industrial merits. Meanwhile, this route can be extended to prepare other functional 2D-MXene materials.

■ ASSOCIATED CONTENT

Ⓢ Supporting Information

Experimental details and comparative data. This material is available free of charge via Internet at http://pubs.acs.org.

■ AUTHOR INFORMATION

Corresponding Author

pengqiuming@gmail.com; zhangqr@ysu.edu.cn

Author Contributions

[#]Qiuming Peng and Jianxin Guo contributed equally.

Notes

The authors declare no competing financial interest.

■ ACKNOWLEDGMENTS

We greatly acknowledge the NSFC (No. 51101142, 50821001, 51102206, and 21207112) NSF of Hebei (No. B2012203060, 13961002D), Program for New Century Excellent Talents in University of Ministry of Education of China (NCET-12-0690), the China Postdoctoral Science Foundation (2013T60265), Foundation for the Excellent Youth Scholars from Universities and Colleges of Hebei Province (No. Y2011113, Y2012019).

■ REFERENCES

(1) Fu, F.; Xie, L.; Tang, B.; Wang, Q.; Jiang, S. *Chem. Eng. J.* **2012**, *189–190*, 283.
(2) (a) Wei, X.; Kong, X.; Wang, S.; Xiang, H.; Wang, J.; Chen, J. *Ind. Eng. Chem. Res.* **2013**, *52*, 17583. (b) Zhang, Q.; Wang, N.; Zhao, L.; Xu, T.; Cheng, Y. *ACS Appl. Mater. Interfaces* **2013**, *5*, 1907.
(3) Zhang, Q.; Du, Q.; Hua, M.; Jiao, T.; Gao, F.; Pan, B. *Environ. Sci. Technol.* **2013**, *47*, 6536.
(4) Mahmoud, A.; Hoadley, A. F. A. *Water Res.* **2012**, *46*, 3364.
(5) Zhang, Q.; Du, Q.; Hua, M.; Jiao, T.; Gao, F.; Pan, B. *Environ. Sci. Technol.* **2013**, *47*, 6536.
(6) Novoselov, K. S.; Geim, A. K.; Morozov, S. V.; Jiang, D.; Zhang, Y.; Dubonos, S. V.; Grigorieva, I. V.; Firsov, A. A. *Science* **2004**, *306*, 666.
(7) Mi, X.; Huang, G.; Xie, W.; Wang, W.; Liu, Y.; Gao, J. *Carbon* **2012**, *50*, 4856.
(8) Chandra, V.; Park, J.; Chun, Y.; Lee, J. W.; Hwang, I.-C.; Kim, K. S. *ACS Nano* **2010**, *4*, 3979.
(9) Tiwari, J. N.; Mahesh, K.; Le, N. H.; Kemp, K. C.; Timilsina, R.; Tiwari, R. N.; Kim, K. S. *Carbon* **2013**, *56*, 173.
(10) Yang, X.; Chen, C.; Li, J.; Zhao, G.; Ren, X.; Wang, X. *RSC Adv.* **2012**, *2*, 8821.
(11) Travlou, N. A.; Kyzas, G. Z.; Lazaridis, N. K.; Deliyanni, E. A. *Langmuir* **2013**, *29*, 1657.
(12) Xu, J.; Wang, L.; Zhu, Y. *Langmuir* **2012**, *28*, 8418.
(13) Lukatskaya, M. R.; Mashtalir, O.; Ren, C. E.; Dall'Agnese, Y.; Rozier, P.; Taberna, P. L.; Naguib, M.; Simon, P.; Barsoum, M. W.; Gogotsi, Y. *Science* **2013**, *341*, 1502.
(14) Naguib, M.; Mashtalir, O.; Carle, J.; Presser, V.; Lu, J.; Hultman, L.; Gogotsi, Y.; Barsoum, M. W. *ACS Nano* **2012**, *6*, 1322.
(15) Mashtalir, O.; Naguib, M.; Mochalin, V. N.; Dall'Agnese, Y.; Heon, M.; Barsoum, M. W.; Gogotsi, Y. *Nat. Commun.* **2013**, *4*, 1716.
(16) Khazaei, M.; Arai, M.; Sasaki, T.; Chung, C. Y.; Venkataramanan, N. S.; Estili, M.; Sakka, Y.; Kawazoe, Y. *Adv. Funct. Mater.* **2013**, *23*, 2185.
(17) Tang, Q.; Zhou, Z.; Shen, P. *J. Am. Chem. Soc.* **2012**, *134*, 16909.
(18) Naguib, M.; Come, J.; Dyatkin, B.; Presser, V.; Taberna, P. L.; Simon, P.; Barsoum, M. W.; Gogotsi, Y. *Electrochem. Commun.* **2012**, *16*, 61.
(19) Hu, Q.; Sun, D.; Wu, Q.; Wang, H.; Wang, L.; Liu, B.; Zhou, A.; He, J. *J. Phys. Chem. A* **2013**, *117*, 14253.
(20) Ma, T. Y.; Zhang, X. J.; Shao, G. S.; Cao, J. L.; Yuan, Z. Y. *J. Phys. Chem. C* **2008**, *112*, 3090.
(21) Choi, J.; Ide, A.; Truong, Y. B.; Kyratzis, I. L.; Caruso, R. A. *J. Mater. Chem. A* **2013**, *1*, 5847.
(22) Hua, M.; Zhang, S.; Pan, B.; Zhang, W.; Lv, L.; Zhang, Q. *J. Hazard. Mater.* **2012**, *211–212*, 317.
(23) Devan, R. S.; Patil, R. A.; Lin, J. H.; Ma, Y. R. *Adv. Funct. Mater.* **2012**, *22*, 3326.
(24) Chen, D.; Cao, L.; Hanley, T. L.; Caruso, R. A. *Adv. Funct. Mater.* **2012**, *22*, 1966.
(25) Mashtalir, O.; Naguib, M.; Dyatkin, B.; Gogotsi, Y.; Barsoum, M. W. *Mater. Chem. Phys.* **2013**, *139*, 147.
(26) Zhang, Q.; Du, Q.; Jiao, T.; Zhang, Z.; Wang, S.; Sun, Q.; Gao, F. *Sci. Rep.* **2013**, *3*, 2551.
(27) Jing, C.; Cui, J.; Huang, Y.; Li, A. *ACS Appl. Mater. Interfaces* **2012**, *4*, 714.
(28) Giammar, D. E.; Maus, C. J.; Xie, L. *Environ. Eng. Sci.* **2007**, *24*, 85.
(29) Brown, G. E., Jr.; Foster, A. L.; Ostergren, J. D. *Proc. Natl. Acad. Sci. U. S. A.* **1999**, *96*, 3388.
(30) Marcus, Y. *J. Chem. Soc., Faraday Trans.* **1991**, *87*, 2995.
(31) Pan, B. C.; Zhang, Q. R.; Zhang, W. M.; Pan, B. J.; Du, W.; Lv, L.; Zhang, Q. J.; Xu, Z. W.; Zhang, Q. X. *J. Colloid Interface Sci.* **2007**, *310*, 99.
(32) Jia, K.; Pan, B. C.; Zhang, Q. R.; Zhang, W. M.; Jiang, P. J.; Hong, C. H.; Pan, B. J.; Zhang, Q. X. *J. Colloid Interface Sci.* **2008**, *318*, 160.
(33) Helfferich, F. *Ion Exchange*; McGraw-Hill: New York, 1963.
(34) Becke, A. D.; Edgecombe, K. E. *J. Chem. Phys.* **1990**, *92*, 5397.